University of Kent

Kent Academic Repository

Zhang, Yukun, Sun, Caiying, Wang, Lijuan and Zhang, Zhen (2026) *Flow Pattern Recognition of CO2 Gas-Liquid Two-Phase Flow Based on Texture Features of Gray-Level Co-occurrence Matrix.* In: 2026 IEEE International Instrumentation and Measurement Technology Conference. . IEEE E-ISBN 979-8-3315-8938-7.

Downloaded from
https://kar.kent.ac.uk/113886/ The University of Kent's Academic Repository KAR

The version of record is available from
https://doi.org/10.1109/I2MTC66907.2026.11694422

This document version
Author's Accepted Manuscript

DOI for this version

Licence for this version
CC BY (Attribution)

Additional information
For the purpose of open access, the author(s) has applied a Creative Commons Attribution (CC BY) licence to any Author Accepted Manuscript version arising.

Versions of research works

Versions of Record
If this version is the version of record, it is the same as the published version available on the publisher's web site. Cite as the published version.

Author Accepted Manuscripts
If this document is identified as the Author Accepted Manuscript it is the version after peer review but before type setting, copy editing or publisher branding. Cite as Surname, Initial. (Year) 'Title of article'. To be published in ***Title of Journal*** , Volume and issue numbers [peer-reviewed accepted version]. Available at: DOI or URL (Accessed: date).

Enquiries
If you have questions about this document contact ResearchSupport@kent.ac.uk. Please include the URL of the record in KAR. If you believe that your, or a third party's rights have been compromised through this document please see our Take Down policy (available from https://www.kent.ac.uk/guides/kar-the-kent-academic-repository#policies).

Flow Pattern Recognition of CO_2 Gas-Liquid Two-Phase Flow Based on Texture Features of Gray-Level Co-occurrence Matrix

1st Yukun Zhang
School of Automation and Electrical Engineering
Inner Mongolia University of Science & Technology
Baotou, China
zyk11011k@163.com

2nd Caiying Sun*
School of Automation and Electrical Engineering
Inner Mongolia University of Science & Technology
Baotou, China
suncaiying2006@163.com

3rd Lijuan Wang
School of Engineering, Mathematics and Physics
University of Kent
Canterbury, UK.
L.wang@kent.ac.uk

4th Zhen Zhang
School of Automation and Electrical Engineering
Inner Mongolia University of Science & Technology
Baotou, China
1729578705@qq.com

***Abstract*—In the field of carbon capture and storage (CCS), accurate recognition of flow patterns in CO_2 gas-liquid two-phase flow is crucial for mass flow rate measurement. This paper presents a flow pattern recognition method based on texture features of gray level co-occurrence matrix (GLCM). This method extracts four GLCM texture features by preprocessing flow pattern images to generate feature vectors, and then uses support vector machine (SVM) model to distinguish three flow patterns in CO_2 gas-liquid two-phase flow: stratified flow, bubbly flow, and mist flow. The experimental results confirm that the proposed method achieves a classification accuracy of 98.14%. The SVM model demonstrates an advantage over both least squares support vector machine (LSSVM) and Back Propagation Neural Network (BPNN) models. This paper provides an accurate and efficient solution for flow pattern recognition in CO_2 gas-liquid two-phase flow.**

Keywords—CCS, CO_2 gas-liquid two-phase flow, flow pattern recognition, GLCM, SVM

I. INTRODUCTION

Carbon capture and storage (CCS) is widely acknowledged as a key technology among those needed to achieve cost-effective, long-term CO_2 mitigation [1]. In CCS, CO_2 may exist in gaseous, liquid, gas-liquid two-phase, or supercritical states. The presence of these different phase states can affect the accuracy of CO_2 mass flow rate measurement, thereby impacting carbon trading accounting and pipeline leakage monitoring during transportation [2, 3].

In terms of traditional flow pattern recognition methods, the recognition technologies based on physical sensors have made significant progress. The techniques such as virtual capacitance tomography combined with numerical simulation have proven effective for oil-gas two-phase flow [4]. Meanwhile, the method utilizing optical probe local parameters [5] or flow-induced vibration signals [6] have proven effective for steam-water two-phase flow conditions. The value of non-invasive methods is well recognized in flow pattern recognition. For instance, a novel approach combining doppler ultrasonic sensors and deep neural networks has been demonstrated for monitoring complex geometries such as S-shaped risers [7]. These methods underscore that multi-sensor information fusion and advanced signal processing are critical for enhancing the accuracy of gas-liquid two-phase flow pattern recognition.

With the rapid development of sensing and imaging technologies, image-based flow pattern recognition methods have attracted increasing attention. By combining high-speed visualization with image processing techniques, spatial and textural information related to gas-liquid interfacial structures can be directly extracted. Recent studies have demonstrated that image-based methods, including convolutional neural networks enhanced with attention mechanisms, can effectively identify flow patterns from two-phase flow images [8]. In addition, recent reviews have highlighted the growing use of artificial intelligence and machine learning techniques for hydrodynamic characterization and flow pattern recognition [9]. Compared with conventional visual inspection, these methods exhibit lower subjectivity and demonstrate stronger adaptability to complex flow conditions. Among these approaches, the support vector machine (SVM) algorithm has been extensively adopted for complex classification tasks, owing to its solid theoretical foundation for handling high-dimensional feature spaces and its favorable generalization properties based on convex quadratic optimization [10]. Moreover, the integration of feature optimization with clustering algorithms has demonstrated significant potential. This combined method of fuzzy C-means clustering and ReliefF attribute weighting enables accurate flow pattern recognition in gas-liquid two-phase flow [11], while similar multi-domain feature frameworks have established the theoretical groundwork for the recognition of gas-liquid two-phase flow patterns in horizontal pipelines [12].

In recent years, Wang et al. [3] integrated flow-pattern recognition into the measurement of CO_2 mass flow rate in CCS transportation pipelines, using the least squares support vector machine (LSSVM) model to identify the flow patterns of CO_2 gas-liquid two-phase flow in horizontal and vertical

Science & Technology Department of Inner Mongolia Autonomous Region.

pipelines. Although this approach relied on flow-induced measurement signals rather than image features, it highlights the engineering relevance of flow pattern identification for CO_2 two-phase flow monitoring. More recently, image-based and data-driven approaches have been explored for CO_2 two-phase flow under controlled experimental conditions. Kadish et al. [13] developed a deep-learning-based computer-vision framework for flow pattern classification in vertical CO_2 two-phase flow using high-speed imaging, covering several typical patterns such as bubbly, slug, churn, annular, and mist-like flows, and reported an average classification accuracy of approximately 92%. Schmid et al. [14] constructed a high-speed visualization database for vertical CO_2 gas-liquid two-phase flow and employed a machine-learning-based classifier to support flow pattern mapping and pattern-transition analysis between different flow patterns in CO_2 gas-liquid two-phase flow, achieving a validated classification accuracy of 95.4% on an independent test set. These studies indicate the feasibility of applying image-based and machine-learning-based methods to CO_2 two-phase flow pattern classification.

Despite these advances, research on image texture analysis and data-driven flow pattern recognition methods in CO_2 gas-liquid two-phase flow is still insufficient under CCS related conditions, especially in horizontal pipeline configurations. Unlike conventional air-water or oil-gas two-phase systems, CO_2 gas-liquid two-phase flow exhibits thermophysical properties that strongly depend on pressure and temperature, including density, compressibility, viscosity, and phase-transition behavior. These inherent characteristics result in significant interfacial fluctuations and flow pattern evolution under high-pressure CCS operating conditions. Consequently, the resulting flow pattern images and their associated texture characteristics differ fundamentally from those observed in classical two-phase flow systems. In this paper, gray-level co-occurrence matrix (GLCM) analysis is employed to extract representative texture features from flow-pattern images, for the quantitative characterization of spatial features linked to different flow patterns, with the SVM classifier adopted as a reliable and interpretable model well suited for experimental and engineering applications where labeled data is limited.

II. METHODOLOGY

The flow pattern recognition framework proposed in this paper comprises three core modules: the preprocessing of images, GLCM feature extraction, and SVM classification. This method integrates image processing techniques with machine learning algorithms, designed to enable high accuracy recognition of flow patterns in CO_2 gas-liquid two-phase flow.

A. The Preprocessing of Images

The purpose of image preprocessing is to optimize the input for the GLCM, thereby extracting high-quality texture features that are closely associated with the intrinsic physical mechanisms of flow patterns.

In pre-processing, RGB images are first converted to grayscale to reduce data dimensionality and computational load, retaining only the luminance information essential for flow structure recognition. Local contrast is then enhanced using contrast-limited adaptive histogram equalization. This technique improves textural visibility by limiting amplification in local regions, thus avoiding the noise and overexposure issues common in global equalization. Finally, to further refine the flow pattern, a morphological opening operation is performed using a circular structural element with a radius of 3 pixels. This method effectively smoothes fine protrusions, suppresses shot noise, and consolidates the continuous regions of the flow patterns while maintaining boundary integrity.

B. GLCM Feature Extraction

The GLCM is a statistical method widely used in image texture analysis, which characterizes image texture properties by quantifying the probability of gray-level values co-occurring in pixel pairs under specific spatial relationships. To obtain a rotation-invariant texture description and capture the inherent anisotropic texture characteristics of CO_2 gas-liquid two-phase flow, this paper calculated the GLCM in four directions of 0°, 45°, 90°, and 135°. The rotation invariance ensures that texture features remain consistent regardless of the flow pattern orientation, thereby enabling reliable classification of CO_2 two-phase flow from arbitrary viewing angles. Although including additional angles could provide finer directional detail, it would introduce redundant computational overhead without substantially improving discriminative power. The rationale for selecting these four directions is as follows:

- 0°: Essential for stratified flow, where the dominant horizontal interface between liquid and gas phases creates strong horizontal texture patterns.
- 45°/135°: Critical for bubbly flow and mist flow, where gas bubbles often align along diagonal turbulence structures, and for mist flow, where randomly dispersed liquid droplets form diagonal clusters due to turbulent eddies.
- 90°: Primarily relevant to stratified flow but irrelevant to mist flow, which exhibits isotropic droplet distribution.

In feature extraction, the pixel distance is set to 1, and the gray level is quantized into 8 levels. Four classic texture features are extracted from the GLCM, including the contrast, correlation, angular second moment, and homogeneity. The arithmetic mean of the feature values in the four directions is taken to form the final four-dimensional feature vectors.

Contrast measures the local gray-level variation intensity in flow pattern images, reflecting texture clarity and groove depth, as shown in (1):

$$Contrast = \sum_{i=1}^{N_g}\sum_{j=1}^{N_g}(i\text{-}j)^2\,P(i,j) \tag{1}$$

where N_g is the total number of gray levels in the image, i denotes the gray level of the starting pixel, j denotes the gray level of the neighboring pixel, and $P(i,j)$ denotes the joint probability of gray levels i and j occurring at a specified spatial offset.

Correlation quantifies the linear dependency between row and column elements in the GLCM, reflecting the directionality and regularity of texture, as shown in (2):

$$Correlation = \frac{\sum_{i=1}^{N_g}\sum_{j=1}^{N_g}(i\text{-}\mu_i)(j\text{-}\mu_j)P(i,j)}{\sigma_i\sigma_j} \tag{2}$$

where μ_i is the row mean, μ_j is the column mean, σ_i is the row standard deviation, and σ_j is the column standard deviation.

Energy (Angular Second Moment, ASM) is the sum of the squares of GLCM elements, reflecting the degree of uniformity in the image texture, as shown in (3):

$$Energy=\sum_{i=1}^{N_g}\sum_{j=1}^{N_g}P(i,j)^2 \tag{3}$$

Homogeneity assesses the local uniformity of the image texture, assigning higher weights to elements near the main diagonal of the GLCM, as shown in (4):

$$Homogeneity=\sum_{i=1}^{N_g}\sum_{j=1}^{N_g}\frac{P(i,j)}{1+(i-j)^2} \tag{4}$$

C. SVM Classification

The SVM model is chosen as the flow pattern classifier due to its well-established theoretical framework, strong generalization capability, and suitability for tasks with limited data. As a classical supervised learning algorithm, the SVM operates by determining an optimal hyperplane to maximize the inter-class geometric margin, thus promoting generalization and helping to prevent overfitting. The primal problem of SVM can be formulated as the following convex quadratic optimization problem, as shown in (5) and (6):

$$min_{w,b,\xi_i}\ \frac{1}{2}\|w\|^2+\frac{1}{2}C\sum_{i=1}^{N}\xi_i \tag{5}$$

$$s.t.\ y_i[w\cdot\varphi(x_i)+b]\geq 1-\xi_i,\xi_i\geq 0,i=1,2,\ldots,N \tag{6}$$

where w is the normal vector of the hyperplane, b is the bias term, ξ_i is the slack variable, C is the regularization parameter controlling the penalty strength for misclassifications, y_i is the true class label, $\varphi(x_i)$ is the feature mapping function, and N is the total number of training samples, which is 865 in this paper.

By introducing Lagrange multipliers and transforming the problem into its dual form for solution, an optimization form that relies solely on the inner products between samples can be obtained, avoiding the explicit computation of the high-dimensional mapping. Ultimately, a classification decision function dependent only on the kernel function between samples is derived, as shown in (7):

$$f(x)=\mathrm{sgn}\left(\sum_{i=1}^{N}\alpha_i y_i K(x_i,x)+b\right) \tag{7}$$

where sgn is the sign function, α_i is the Lagrange multipliers obtained from the SVM optimization, x represents a new sample to be classified. x_i is the i-th training sample, y_i is the true class label of the i-th training sample, K is the kernel function symbol, b is the bias term.

The radial basis function (RBF) kernel is employed in the SVM model to capture fine-grained variations in image data. Its implicit mapping via the kernel trick efficiently processes high-dimensional features extracted by the GLCM, while the bandwidth parameter σ controls the trade-off between model complexity and generalization performance, ensuring robust flow pattern recognition in CO_2 gas-liquid two-phase flow.

III. Flow Pattern Analysis

The physical mechanisms for three typical CO_2 gas-liquid flow patterns are analyzed in relation to their texture signatures, providing a physically grounded interpretation for the subsequent experimental results.

A. Stratified Flow Analysis

In the CO_2 gas-liquid two-phase flow, when the flow velocities of both the gas phase and the liquid phase are relatively low, gravity governs the phase separation process, resulting in a distinct, smooth, and stable gas-liquid interface. Under such conditions, both phases remain continuous media, constituting a typical continuous-continuous flow pattern. In horizontal circular pipes, this flow pattern typically manifests as a stable stratified structure with the liquid phase at the bottom and the gas phase at the top. When small-amplitude undulations develop along the interface, it is classified as wavy flow. Given that the two exhibit visually similar textures and share the same underlying physical mechanism, this paper groups them into a unified stratified flow class. The image of stratified flow is shown in Fig. 1.

In stratified flow, the formation of large-area, smooth, and stable stratified regions between the gas and liquid phases in a horizontal pipe results in a highly uniform gray-level distribution in the image, where adjacent pixel values are very similar. This structural characteristic concentrates the probability mass of the GLCM near its main diagonal, leading to a high homogeneity value. Due to the frequent occurrence of specific gray-level pairs in the flow pattern image results in a concentrated distribution of elements in the GLCM, thereby producing a significantly high energy value. The smooth gas-liquid interface lacks abrupt gray-level transitions, resulting in generally small differences between pixel pairs and consequently a low contrast value. It is noteworthy that the stratified structure extends axially along the pipe, exhibiting distinct directionality. This imparts a strong linear gray-level dependence in the GLCM calculated at 0° or 180°, resulting in a relatively high correlation value.

B. Bubbly Flow Analysis

The bubbly flow is formed by the dispersion of the gas phase into fine bubbles within the continuous liquid phase following a moderate increase in gas velocity. Buoyancy-driven bubbles migrate upward and accumulate in the upper part of the pipe in a liquid-continuous, gas-dispersed flow, while maintaining the macroscopic continuity of the flow due to their liquid-surrounded state. The image of the bubbly flow is shown in Fig. 2.

In the bubbly flow, the gas phase is dispersed as discrete bubbles within the continuous liquid phase. Each bubble edge forms a local gas-liquid interface, creating distinct gray-level gradients that raise contrast above stratified flow, yet the bubbles' limited size and uniform liquid background prevent gray-level variation from reaching mist-flow intensity, keeping contrast at a moderate level. While the continuous liquid phase maintains texture uniformity in bubbly flow images, yet the scattered bubbles introduce local disturbances that weaken global consistency, thus yielding intermediate homogeneity and energy values between those of stratified flow and mist flow. Furthermore, randomness in the spatial distribution, size, and shape of the bubbles results in a marked decrease in the directional correlation.

C. Mist Flow Analysis

The mist flow is formed when the CO_2 gas phase velocity is high enough to shatter the liquid into fine droplets, resulting in a gas-continuous, liquid-dispersed pattern characterized by high turbulence, transient interfaces, and random spatial distribution of phases. The image of mist flow is shown in Fig. 3.

In the mist flow, the liquid phase is shattered by the high-velocity gas stream into a multitude of fine droplets that are randomly dispersed throughout the gas phase. This results in dense and disordered high-frequency gray-level transitions within the image, thereby driving the contrast to its maximum value. Owing to the extreme randomness of the texture, the occurrence probability of any gray-level combination tends toward uniformity. Energy and homogeneity are significantly reduced due to the widely distributed elements of the GLCM. This flow pattern lacks any distinct dominant direction or periodic structure. Gray-level variations in all directions exhibit only weak linear dependence, which causes the correlation to approach its theoretical lower limit.

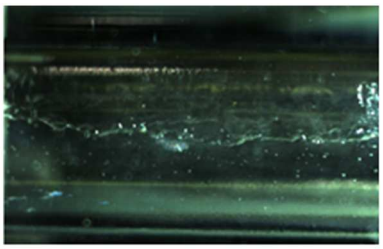


Fig. 1. Stratified Flow



Fig. 2. Bubbly Flow

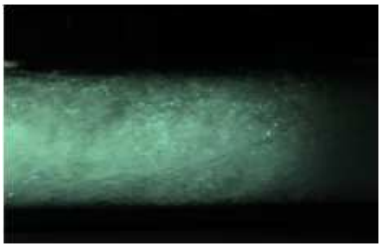


Fig. 3. Mist Flow

IV. Experiment and Result Analysis

A. Equipment and Data

The experiments were conducted on a high-pressure CO_2 gas-liquid two-phase flow experimental platform, as shown in Fig. 4. By regulating the operating pressure, temperature, and gas-liquid mass flow rate, stable CO_2 gas-liquid two-phase flow conditions can be established in the experimental pipeline, enabling the formation of different flow patterns under controlled laboratory conditions. The flow pattern image acquisition pipe section is a horizontal stainless-steel pipe with an inner diameter of 25 mm. The experiments were carried out at temperatures between 18 and 30 °C and pressures ranging from 5.4 to 7.2 MPa. The gas-phase and liquid-phase mass flow rate were controlled within the ranges of 10-300 kg/h and 300-2700 kg/h, respectively. Variations in these operating parameters resulted in markedly distinct thermodynamic and interfacial dynamic states, thereby giving rise to physically distinct two-phase flow patterns.

Flow-pattern images were captured through an observation window mounted on the horizontal pipe section, where the flow pattern acquisition system was installed as illustrated in Fig. 5. This system was composed of a light source, a high-speed camera and a high-definition observation window, enabling clear visualization of the gas-liquid interfacial structures. As a result, despite the fixed pipe geometry, the acquired flow-pattern images exhibited substantial physical diversity and were not highly correlated.

Based on the above experimental platform and operating conditions, a flow pattern image database was constructed using real images acquired under controlled laboratory conditions. By carefully adjusting the operating parameters, three typical flow patterns, namely stratified flow, bubbly flow, and mist flow, were formed and captured. In total, 1080 flow pattern images were collected, with 360 images corresponding to each flow pattern. All images were manually labeled according to the observed flow patterns and subsequently divided into a training set and a test set using an 8:2 ratio. This data partitioning strategy provides sufficient samples for model learning and parameter optimization, while reserving an independent test set for an objective evaluation of the generalization performance of the proposed method.

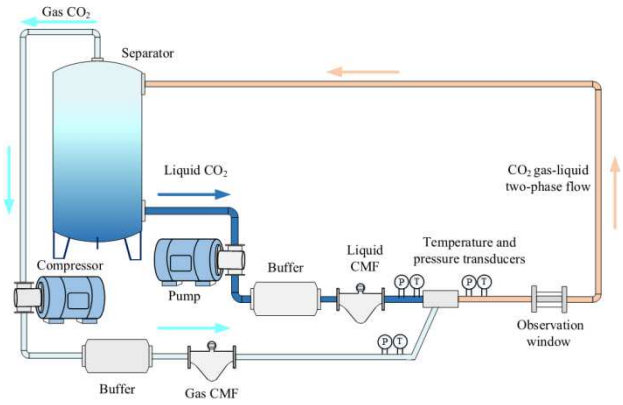


Fig. 4. CO_2 gas-liquid two-phase flow experimental platform

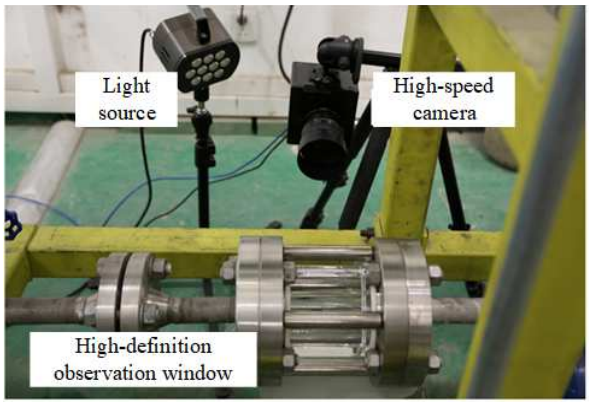


Fig. 5. Flow pattern acquisition system

B. Model Training

In the feature preprocessing phase, Z-score standardization was applied to the 4-dimensional GLCM feature vectors of the training set, with the same mean and standard deviation used to standardize the features of the test set to ensure consistent data distribution.

Hyperparameter optimization was carried out using grid search-combined with 5-fold cross-validation. The search was conducted over an exponential parameter space defined by the penalty parameter C □ [0.1, 1, 10, 100] and the RBF kernel width parameter σ □ [0.1, 1, 10, 100], yielding a total of 16 parameter combinations. The regularization parameter C serves to balance the trade-off between tolerance for training error and decision-boundary complexity, whereas the kernel width σ dictates the influence range of individual training samples in the feature space.

The optimization results indicated that the model achieved the highest cross-validation accuracy when the penalty parameter C was set to 10.0 and the RBF kernel width σ was set to 1.0. The performance variation of the model across all 16 parameter combinations evaluated in the grid search is illustrated in Fig. 6. In the figure, the horizontal axis displays the 16 different parameter combinations in sequentially numbered order, while the vertical axis shows four performance metrics, expressed as percentages. It is notable that all four performance curves vary in unison across the parameter grid and simultaneously peak at the same combination.

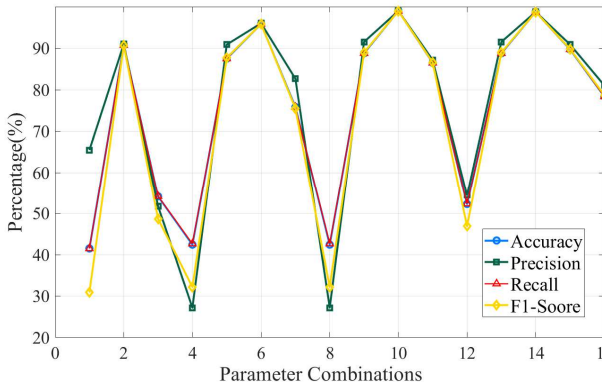


Fig. 6. Performance Comparison of Parameter Combinations

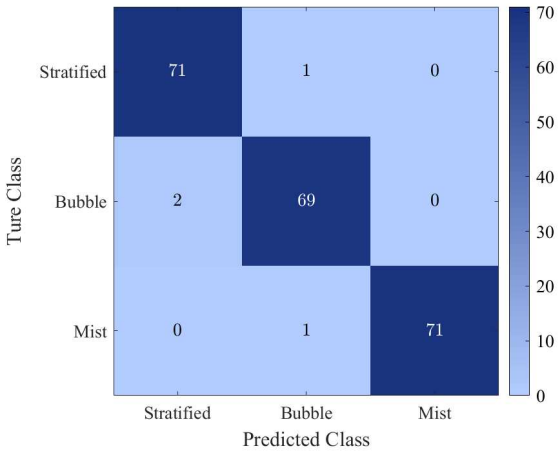


Fig. 7. Confusion matrix of flow pattern classification

As shown in Fig. 6, all performance curves exhibit significant fluctuations with varying parameters, indicating that the model demonstrates notable sensitivity to hyperparameter selection. Notably, all four curves reach their peaks at the same parameter combination. In contrast, performance under other parameter settings declines to varying degrees. This visualization visually confirms that the optimal hyperparameters determined through grid search achieve the best trade-off between model complexity and generalization capability.

C. Result Analysis

The model achieved an average classification accuracy of 98.14 % on the independent test set, demonstrating its accuracy and generalization capability in flow pattern recognition. The detailed classification results are presented in Fig. 7.

The model achieved the recognition accuracies of 98.6% for stratified flow, 97.2% for bubbly flow, and 98.6% for mist flow. These results confirm that, within the SVM framework, the selected feature space and hyperparameter optimization are effective, thereby fulfilling the requirements for high-precision flow pattern recognition.

D. Comparative Experiments and Analyses

To verify the performance of the proposed method, its flow pattern classification results were compared with those of the LSSVM and Back Propagation Neural Network (BPNN) models using the same GLCM features, as shown in Table I.

The experimental results indicate that the SVM model outperforms the other two classifiers across all evaluation metrics. Its accuracy, precision, recall, and F1-score all exceed 98%, delivering an outstanding and well-balanced overall performance. Although the LSSVM model also employs a kernel-based approach, its least-squares loss function is more sensitive to noise and outliers, which may lead to slightly inferior generalization on the dataset used in this study. As for the BPNN model, a type of multilayer perceptron, its nonlinear modeling capability cannot be fully leveraged when processing the GLCM features in this research. Moreover, it is more susceptible to influences from parameters such as initial weights and learning rates, resulting in less stable convergence and consequently a relatively lower recognition rate compared to the SVM model.

TABLE I. COMPARISON OF PERFORMANCE

Classifier	Accuracy (%)	Precision (%)	Recall (%)	F1-score (%)
SVM	98.14	98.15	98.13	98.14
LSSVM	93.02	93.98	93.06	93.09
BPNN	85.58	86.90	85.53	85.71

While modern deep learning models (e.g., convolutional neural networks and transformer-based architectures) deliver state-of-the-art results in large-scale image recognition, their application typically requires extensive labeled datasets and substantial computational resources. In practical CCS monitoring and experimental environments, constraints such as limited data availability, real-time processing requirements, computational resource limitations, and model interpretability must be considered. Therefore, the objective of this paper is to develop a lightweight, stable, and field-deployable flow pattern recognition approach rather than to pursue state-of-the-art performance on benchmark image datasets. Under these conditions, the SVM and LSSVM models offer a favorable balance between recognition performance, robustness, and computational efficiency, while the BPNN is adopted as a representative classic neural network model for baseline comparison in Table I.

V. CONCLUSION

This paper proposes a flow pattern recognition method for CO_2 gas-liquid two-phase flow based on GLCM texture features and the SVM classifier. Under CCS-relevant operating conditions, CO_2 gas-liquid two-phase flow experiments were conducted, and a flow-pattern image database covering a wide range of pressure, temperature, and mass flow rate conditions was constructed in the high-pressure CO_2 pipeline. Four representative GLCM texture features are extracted from flow pattern images to characterize the spatial textures of three typical flow patterns, namely stratified flow, bubbly flow, and mist flow, and are subsequently used as inputs to the SVM model with optimized hyperparameters. Experimental validation on an independent test set demonstrates that the proposed method achieves an average classification accuracy of 98.14%, outperforming other benchmark classifiers and confirming its high accuracy and robustness. These results indicate that the proposed GLCM-SVM framework provides a reliable and effective solution for flow pattern recognition in CO_2 gas-liquid two-phase flow under CCS conditions.

Deep learning models, including convolutional neural networks and transformer-based architectures, have demonstrated strong potential for image-based flow pattern recognition. As larger-scale experimental datasets become available, these models will be investigated in our future work. Furthermore, future experiments will extend the current database by employing test facilities with different pipe diameters and orientations, so as to further evaluate the generalization ability and robustness of the proposed method under various CO_2 two-phase flow pipeline conditions.

ACKNOWLEDGMENT

This work was supported by the Science & Technology Plan Project of Inner Mongolia Autonomous Region (No. 2025YFHH0059). The authors would also like to acknowledge the support provided by the Institute for Multiphase Flow Measurement and Combustion Process Monitoring Technology of North China Electric Power University (Beijing), where the research team led by Academician Yong Yan is affiliated, for the CO_2 flow pattern experiments.

REFERENCES

[1] Y. W. Zheng, L. Gao, S. He and H. G. Jin, "Reduction potential of the energy penalty for CO_2 capture in CCS," Frontiers in Energy, vol. 17, pp. 390-399, February 2023.

[2] C. Y. Sun, Y. Yan, W. B. Zhang and D. Shao. "Measurement of CO_2 leakage from pipelines under CCS conditions through acoustic emission detection and data driven modeling," Measurement, vol. 237, September 2024.

[3] L. J. Wang, Y. Yan, X. Wang, T. Wang, Q. S. Duan and W. B. Zhang, "Mass flow measurement of gas-liquid two-phase CO_2 in CCS transportation pipelines using Coriolis flowmeters," International Journal of Greenhouse Gas Control, vol. 68, pp. 269-275, January 2018.

[4] Y. Xu, H. Pu, Y. Li and H. G. Wang. "Flow pattern identification for gas-oil two-phase flow based on a virtual capacitance tomography sensor and numerical simulation," Flow Measurement and Instrumentation, vol. 92, August 2023.

[5] T. Wang, Z. H. Liu, M. Gui, Q. C. Bi and Z. Q. Sui, "Flow regime identification of steam-water two-phase flow using optical probes, based on local parameters in vertical tube bundles," Flow Measurement and Instrumentation, vol. 79, June 2021.

[6] F. D. Carvalho, M. D. Figueiredo and A.L. Serpa, "Flow pattern classification in liquid-gas flows using flow-induced vibration," Experimental Thermal and Fluid Science, vol. 112, April 2020.

[7] S. G. Nnabuife, B. Kuang, J. F. Whidborne and Z. Rana, "Non-Intrusive Classification of Gas-Liquid Flow Regimes in an S-shaped Pipeline Riser Using a Doppler Ultrasonic Sensor and Deep Neural Networks," Chemical Engineering Journal, vol. 403, January 2021.

[8] W. L. Qiao, H. T. Y. Guo, E. Z. Huang, H. Q. Chen and C. P. Lian, "Two-phase flow pattern identification by embedding double attention mechanisms into a convolutional neural network," Journal of Marine Science and Engineering, pp. 793, April 2023.

[9] J. A. Gomez Camperos, M. M. Hernández Cely and A. Pardo García, "Artificial Intelligence Techniques for the Hydrodynamic Characterization of Two-Phase Liquid-Gas Flows: An Overview and Bibliometric Analysis," Fluids, vol. 7, July 2024.

[10] J. Cervantes, F. Garcia-Lamont, L. Rodríguez-Mazahua and A. Lopez, "A comprehensive survey on support vector machine classification: Applications, challenges and trends," Neurocomputing, vol. 408, pp.189-215, September 2020.

[11] L. M. Pan, M. H. Zhang, P. Ju, H. He and M. Ishii, "Vertical co-current two-phase flow regime identification using fuzzy C-means clustering algorithm and ReliefF attribute weighting technique," International Journal of Heat and Mass Transfer, vol. 95, pp.393-404, April 2016.

[12] F. Dong, S. Zhang, X. W. Shi, H. Wu and C. Tan, "Flow regimes identification-based multidomain features for gas-liquid two-phase flow in horizontal pipe," IEEE Transactions on Instrumentation and Measurement, vol. 70, pp. 1-11, June 2021.

[13] S. Kadish, D. Schmid, J. Son and E. Boje, "Computer vision-based classification of flow regime and vapor quality in vertical two-phase flow," Sensors, vol. 22, pp. 996, June 2021.

[14] D. Schmid, B. Verlaat, P. Petagna, R. Revellin and J. Schiffmann, "Flow pattern observations and flow pattern map for adiabatic two-phase flow of carbon dioxide in vertical upward and downward direction," Experimental Thermal and Fluid Science, vol. 131, February 2022.